https://doi.org/10.5194/amt-2024-33
Preprint. Discussion started: 12 March 2024

Atmospheric Measurement Techniques Discussions

Diurnal variations of NO_2 tropospheric vertical column density over the Seoul Metropolitan Area from the Geostationary Environment Monitoring Spectrometer (GEMS): seasonal differences and impacts of varying *a priori* NO_2 profile data

Seunghwan Seo[1], Si-Wan Kim[1,2*], Kyoung-Min Kim[1], Andreas Richter[3], Kezia Lange[3], John P. Burrows[3], Junsung Park[4**], Hyunkee Hong[5], Hanlim Lee[4], Ukkyo Jeong[4], and Jhoon Kim[1*]

[1]Department of Atmospheric Sciences, Yonsei University, Seoul, Republic of Korea

[2]Irreversible Climate Change Research Center, Yonsei University, Seoul, Republic of Korea

[3]Institute of Environmental Physics, University of Bremen, Bremen, Germany

[4]Division of Earth Environmental System Science, Major of Spatial Information Engineering, Pukyong National University, Busan, Republic of Korea

[5]National Institute of Environmental Research, Incheon, Republic of Korea

*To whom correspondence should be addressed:

Si-Wan Kim (e-mail: siwan.kim@yonsei.ac.kr) and Jhoon Kim (e-mail: jkim2@yonsei.ac.kr).

**now at: Center for Astrophysics | Harvard & Smithsonian, Cambridge, MA, USA

https://doi.org/10.5194/amt-2024-33
Preprint. Discussion started: 12 March 2024

Atmospheric Measurement Techniques Discussions

Abstract

Geostationary Environment Monitoring Spectrometer (GEMS), launched in 2020, provides both temporally and spatially continuous air quality data from geostationary Earth orbit (GEO). In this study, we analyzed seasonal characteristics of GEMS tropospheric NO_2 vertical column density (NO_2 TropVCD) diurnal patterns and impacts of *a priori* data from diverse chemical transport model (CTM) simulations over the Seoul Metropolitan Area (SMA), using the GEMS products retrieved by the IUP algorithm. We found that both the amounts of NO_2 TropVCD and the peak time vary according to the season – the maximum value occurs earlier in July (10 KST) compared to other months (12 KST), with relatively lower value ($8.53 – 9.81 \times 10^{15}$ molec. cm^{-2}). In wintertime, the decrease in NO_2 TropVCD over time was relatively slower than in summertime. Also, we examined the impact of changes in *a priori* data on the GEMS NO_2 TropVCD. When we compare GEMS NO_2 data retrieved with default NO_x emissions and uniformly 20%-reduced NO_x emissions, there are no notable discrepancies as simulated NO_2 profiles from CTM are nearly identical over the SMA. However, when the vertical profile at 06:45 UTC (13:45 KST) was applied for retrievals at all times, there are 11.9 – 16.1% lower values before 13:45 KST and up to 4.9% higher values after 13:45 KST compared to the control run case. Our study highlighted two key findings: (1) GEMS NO_2 products describe distinct seasonal features, including the absolute values (highest in January and lowest in July) and diurnal patterns (persisting longer in January and declining rapidly in July), (2) changes of *a priori* data have the impacts of up to 19.2% on the GEMS NO_2 TropVCD.

https://doi.org/10.5194/amt-2024-33
Preprint. Discussion started: 12 March 2024

Atmospheric Measurement Techniques Discussions

1. Introduction

Nitrogen dioxide (NO_2) is one of the most important trace gases involved in photochemical reactions related to tropospheric ozone chemistry (Milford et al., 1989). In recent decades, environmental satellites such as GOME, OMI, SCIAMACHY, and TROPOMI have observed tropospheric NO_2 vertical column densities (TropVCDs) from space (Burrows et al., 1999, Levelt et al., 2006, Bovensmann et al., 1999, Veefkind et al., 2012), which have been extensively utilized for detection of various nitrogen oxides sources, emissions estimates, and probing related chemistry across the globe. While these low Earth orbit (LEO) satellites provide spatially continuous data, observations are obtained only once or twice per day. The Geostationary Environment Monitoring Spectrometer (GEMS), launched in 2020, produces not only spatially but also temporally continuous air quality data over Asia from the geostationary Earth orbit (GEO) (J. Kim et al., 2020). GEMS provides diurnal variations of NO_2 TropVCD, enabling analysis of seasonal changes not only in pollutant concentration but also in temporal characteristics such as peak times and processes of accumulation and loss, which vary by season.

In the process of NO_2 data retrieval, air mass factors (AMF) are used to convert slant column density (SCD) to VCD (Palmer et al., 2001). Lorente et al. (2017) reported that AMF calculation is the largest source of uncertainty in NO_2 satellite retrievals, especially with varying ancillary data such as surface albedo, terrain height, cloud parameters, and trace gas profiles. Therefore, selecting appropriate *a priori* data is necessary to accurately retrieve VCDs from satellite observations.

This study investigates two aspects of GEMS NO_2 TropVCD data over the Seoul Metropolitan Area (SMA): (1) seasonal variations and (2) the impact of *a priori* profiles on the retrieved GEMS NO_2 TropVCDs. In Section 3.1, we utilized two chemical transport models (CTM) – Weather Research and Forecast model combined with Chemistry (WRF-Chem) and the global chemistry transport model TM5 (Tracer Model

https://doi.org/10.5194/amt-2024-33
Preprint. Discussion started: 12 March 2024


Atmospheric Measurement Techniques Discussions

5) to analyze both seasonal variations and *a priori* data impacts. Changes in values and peak times according to the seasons were analyzed. Differences in spatial distributions of NO_2 TropVCD between the two GEMS datasets that utilized different *a priori* data were identified for each season and time. In Section 3.2, we compared three GEMS datasets retrieved with different *a priori* data from the WRF-Chem model. This study includes the impacts of both NO_x emission inventories and vertical distributions on NO_2 TropVCDs.

2. Data and methods

2.1. GEMS products

GEMS is an ultraviolet-visible (UV-VIS) instrument with the spectral coverage of 300 – 500 nm with 0.6 nm spectral resolution (J. Kim et al., 2020). The nominal spatial resolution is 3.5 km × 7.7 km for gases including NO_2. The overall field of regard (FOR) of GEMS covers 75° – 145°E longitude and 5°S – 45°N latitude. GEMS measures hourly during the daytime. The number of observations varies depending on the months – for South Korea, observations are least frequent in January, with six observations per day, and most frequent from April to September, with ten observations per day. We utilized GEMS NO_2 TropVCD data with the IUP algorithm (GEMS IUP products) in January, April, July, and October 2021 – detailed explanations of GEMS IUP products are shown in Section 2.1.1.

2.1.1. GEMS IUP products

The GEMS NO_2 vertical columns used in this study are from the scientific data product of the University of Bremen, version 0.9. This is an early version of the product described in Richter et al., 2024 which was still without cloud correction. NO_2 slant columns are retrieved in the large fitting window 405 – 485nm to reduce noise. In

https://doi.org/10.5194/amt-2024-33
Preprint. Discussion started: 12 March 2024

Atmospheric Measurement Techniques Discussions

addition to the cross-sections of other absorbing species (O_3, O_4, H_2O and liquid water) pseudo cross-sections for the Ring effect, for GEMS instrument polarization sensitivity and the effects of scene inhomogeneity are included. The stratospheric correction is performed using a variant of the algorithm described in Beirle et al., 2016 called STREAM-B. Conversion to vertical tropospheric columns is based on look-up tables of altitude dependent air mass factors calculated with the radiative transfer model SCIATRAN (Rozanov et al., 2014) using LER surface reflection values from the OMI minimum reflectivity data base (Kleipool et al., 2008). The temperature dependence of the NO_2 absorption is corrected in the air mass factor calculation as proposed in Boersma et al., 2004. The NO_2 a priori data used varies between the different runs as described below.

2.2. *a priori* data

2.2.1. WRF-Chem

We utilized WRF-Chem v4.4, developed by the National Oceanic and Atmospheric Administration (NOAA) and National Center for Atmospheric Research (NCAR), to generate *a priori* data for this study (Grell et al., 2005, Skamarock et al., 2021). The chemistry scheme is selected to the Regional Atmospheric Chemistry Mechanism (RACM) with Secondary Organic Aerosol-Volatility Basis Set (SOA-VBS) option (chem_opt = 108) (Ahmadov et al., 2012). The horizontal resolution of WRF-Chem simulation is 28 km × 28 km, with 59 customized vertical layers. Detailed model configuration is described in Kim et al. (2023). To cover the stratospheric vertical profiles, the Whole Atmosphere Community Climate Model (WACCM) model outputs were combined to the WRF-Chem data (ACOM/NCAR/UCAR, 2020, last access: 05 Dec 2022). The combined data comprises a total of 113 vertical layers. For the emission inventory, EDGAR-HTAP v3 (Crippa et al., 2023) was utilized for all WRF-Chem model simulations in this study. A diurnal factor was applied to EDGAR-HTAP v3,

https://doi.org/10.5194/amt-2024-33
Preprint. Discussion started: 12 March 2024


Atmospheric Measurement Techniques Discussions

shifting the values obtained from the Los Angeles Basin in Kim et al. (2016) by one hour. We set three different cases, WRF-Chem v2, f2, and v3, to analyze impacts of *a priori* data on NO_2 TropVCD retrievals – **Table 1** lists the cases defined. WRF-Chem v2 served as the control run, using EDGAR-HTAP v3. The model outputs of WRF-Chem f2 case is as same as WRF-Chem v2, but only 04:45 UTC (13:45 KST) data are used for calculating air mass factor. WRF-Chem v3 used EDGAR-HTAP v3, but NO_x emissions are reduced by 20% for whole domain. The comparison between WRF-Chem v2 and v3 will explore the impact of NO_x emissions on NO_2 TropVCDs, while the comparison between WRF-Chem v2 and f2 will reveal the changes resulting from the different vertical profiles.

2.2.2. TM5

TM5 is a global three-dimensional atmospheric chemistry transport model (Huijnen et al., 2010), evolved from the original TM2 model (Heimann et al., 1988). The meteorological data for TM5 simulations are obtained from the European Centre for Medium-Range Weather Forecasts (ECMWF) operational forecast data. TM5 model outputs have the horizontal resolution of 1° × 1°, and 34 vertical layers. We used NO_2 profiles from the TM5-MP chemistry transport model (Huijnen et al., 2010; Williams et al., 2017) run performed for the TROPOMI operational product. The data are available at 30 minutes time resolution.

3. Diurnal profiles of GEMS NO_2 TropVCD

3.1. Seasonal variations

Figure 1 displays diurnal profiles of NO_2 TropVCD from GEMS products with *a priori* data from WRF-Chem v3 and TM5 for January, April, July, and October 2021 over the SMA (126.5° – 127.3°E, 37.2° – 37.8°N). Both products exhibit similar diurnal

https://doi.org/10.5194/amt-2024-33
Preprint. Discussion started: 12 March 2024


Atmospheric Measurement Techniques Discussions

variations across all months, with increasing trends observed during the morning followed by a decrease in VCDs. The peak time is earliest in July (10 KST), while for other months, the daily maximum values occur at 12 KST. Daily mean and maximum concentrations are highest in January (17.02 – 19.36 × 10^{15} molec. cm^{-2}), October (13.20 – 15.47 × 10^{15} molec. cm^{-2}), April (12.59 – 13.59 × 10^{15} molec. cm^{-2}), and July (8.53 – 9.81 × 10^{15} molec. cm^{-2}) in that order. Differences in photochemical reaction rates may affect changes in NO_2 TropVCD for each month. Shah et al. (2020) mentioned that the lifetime of NO_x in the boundary layer mainly determines seasonal variation of NO_2 columns. Longer lifetime can also affect the time when the maximum value appears – since NO_x loss processes occur more slowly in winter, NO_2 accumulates for a longer period, therefore the peak time appears later than in summer; Yang et al. (2023) also reported that the diurnal pattern of total NO_2 column is mainly driven by chemistry in summer.

VCD differences between the two GEMS products appeared as similar values throughout the observation period. The largest difference between the two retrievals is found in January (2.05 – 2.75 × 10^{15} molec. cm^{-2}, 13.3 – 18.0%), while the smallest difference occurs in July (0.25 – 1.40 × 10^{15} molec. cm^{-2}, 4.3 – 19.2%). Spatial maps for differences of NO_2 TropVCD retrieved between the two products are shown in **Figure 2**. For the whole times, GEMS NO_2 TropVCDs with WRF-Chem v3 data are retrieved higher than those with TM5 data over SMA (pink box) and its downwind region (southeast of SMA). The coarser horizontal resolution of the TM5 model would be one of the reasons why these differences occur – NO_2 profiles over polluted urban areas are diluted with relatively clean rural conditions in the large horizontal grids. Those differences develop during the morning and diminish after noon. In January and October, differences over SMA regions remain until 15 ~ 16 KST, while the differences almost disappeared after 15 KST in July.

https://doi.org/10.5194/amt-2024-33
Preprint. Discussion started: 12 March 2024


Atmospheric Measurement Techniques Discussions

However, the differences in GEMS NO_2 TropVCD caused by *a priori* data are much smaller than the differences in model TropVCD themselves. **Figure 3** represents diurnal profiles of model-simulated NO_2 TropVCD for the same period and location of **Figure 1**. Unlike the GEMS products, there are huge differences between the two model products, not only concerning their absolute values but also their diurnal patterns. For all four months, WRF-Chem v3 shows overall increasing trends of TropVCD while TM5 simulates opposite patterns. Curtain plots of model vertical NO_2 profiles from WRF-Chem v3 and TM5 over SMA are shown in **Figure 4**. In WRF-Chem v3 (upper figures), high NO_2 concentrations remain during the afternoon, although vertical mixing occurred up to the 750 hPa level in July, transporting abundant amounts of NO_2 aloft. In TM5, on the other hand, NO_2 concentration was dropped below 5 ~ 10 ppbv in the afternoon. Therefore, the differences between WRF-Chem v3 and TM5 increase during the day (**Figure 3**), but in the GEMS data, there are no substantial differences between the two products (**Figure 1**).

3.2. Sensitivity to *a priori* data

Figure 5 compares the diurnal profiles of GEMS NO_2 TropVCD with *a priori* data from WRF-Chem v2, f2, and v3 during October 25 – 28, 2021 over the SMA. All three data sets exhibit identical diurnal patterns, similar to those shown in **Figure 1**. Although WRF-Chem v2 and v3 have 20% differences in NO_x emissions, the two GEMS data show minimal differences ($0.15 – 0.59 \times 10^{15}$ molec. cm^{-2}) throughout the observations, as the model NO_2 TropVCDs from WRF-Chem v2 and v3 are nearly identical (**Figure 6**). However, a comparison of WRF-Chem v2 and f2 reveals substantial disparities – WRF-Chem f2 shows lower VCDs before 14 KST and higher VCDs after 14 KST. **Figure 7** displays diurnal variations of AMF from WRF-Chem v2, f2, and v3. Since WRF-Chem f2 utilized *a priori* values from WRF-Chem v2 at 04:45 UTC (13:45 KST)

https://doi.org/10.5194/amt-2024-33
Preprint. Discussion started: 12 March 2024


Atmospheric Measurement Techniques Discussions

to calculate AMF for all times, WRF-Chem f2 shows almost no temporal variations in AMF. Conversely, air mass factors from WRF-Chem v2 and v3 show lower values than those from WRF-Chem f2 during the morning time and higher values after 14 KST. Therefore, NO_2 TropVCDs calculated using WRF-Chem f2 show 11.9 – 16.5% lower values before 13:45 KST and up to 4.9% higher values after 13:45 KST compared to those using WRF-Chem v2. Notably, despite the diverse diurnal variations in *a priori* data, the retrieved columns based on different *a priori* data exhibited similar diurnal patterns that do not align with any specific *a priori* data, as shown in Section 3.1 (**Figure 1** and **Figure 3**). Although WRF-Chem v3 shows up to 12.6 times higher NO_2 TropVCD than TM5 in July, the differences in AMF between WRF-Chem v3 and TM5 for July are 5.5 – 16.4% (**Figure 8**).

4. Conclusions

In this study, we analyzed seasonal variations of retrieved GEMS NO_2 TropVCDs using the IUP algorithm and the impacts of *a priori* profiles on the NO_2 VCD retrievals. GEMS NO_2 products exhibit notable changes in the amounts and peak times of NO_2 columns over different times and seasons. Higher concentrations of NO_2, with peak times occurring later, are observed in January compared to July, with gradual declines during the afternoon. This finding is consistent with previous studies based on surface observations and modeling, such as H. C. Kim et al. (2020). Distinct diurnal patterns observed according to the season suggest variations in NO_x lifetime due to different photochemical conditions. Further research is required to estimate NO_x emissions and lifetimes using satellite products. However, different *a priori* profiles with varying NO_x emissions and vertical profiles have only a minimal impact on NO_2 TropVCD retrievals; there are negligible changes in the retrieved columns when NO_x emissions are reduced by 20% over the entire domain, and decreases of up to 16.5% in the columns when vertical profiles are fixed to a single profile at 04:45 UTC (13:45 KST). Retrieved NO_2

https://doi.org/10.5194/amt-2024-33
Preprint. Discussion started: 12 March 2024


Atmospheric Measurement Techniques Discussions

TropVCD diurnal patterns are not heavily influenced by the *a priori* data – despite their *a priori* data exhibiting contrasting diurnal patterns, the diurnal variations of the three different retrievals showed similar patterns. Therefore, uncertainties arising not only from *a priori* NO_2 profiles but also other factors such as cloud screening, aerosol impacts, and geometric information should be considered in satellite retrievals, as emphasized by previous studies such as Lorente et al. (2017) or Hong et al. (2017), which highlight the importance of cloud parameters, aerosol characteristics, and surface albedo.

Data availability

GEMS measurement data retrieved by the IUP algorithm are available on request from Andreas Richter (richter@iup.physik.uni-bremen.de).

Author contributions

SWK initiated this study and secured funding. SS and SWK analyzed the satellite and model data. SS, KMK, and SWK conducted the model simulations. AR, KL, and JPB provided GEMS IUP products and analyzed the data. JK, JP, HH, HL, UJ retrieved and analyzed the GEMS observations and discussed the results. SS and SWK wrote the paper, with contributions from all co-authors.

Competing interests

At least one of the authors is a member of the editorial board of Atmospheric Measurement Techniques.

https://doi.org/10.5194/amt-2024-33
Preprint. Discussion started: 12 March 2024

Atmospheric Measurement Techniques Discussions

Acknowledgement

This work was supported by the National Research Foundation of Korea (NRF) grant funded by the Korea government (MSIT) (No. 2020R1A2C2014131). All the computing resources are provided by National Center for Meteorological Supercomputer.

References

Ahmadov, R., McKeen, S. A., Robinson, A. L., Bahreini, R., Middlebrook, A. M., de Gouw, J. A., Meagher, J., Hsie, E.-Y., Edgerton, E., Shaw, S., and Trainer, M., A volatility basis set model for summertime secondary organic aerosols over the eastern United States in 2006, *J. Geophys. Res. Atmos.*, 117, D06301, 2012, https://doi.org/10.1029/2011JD016831.

Atmospheric Chemistry Observations & Modeling/National Center for Atmospheric Research/University Corporation for Atmospheric Research, Whole Atmosphere Community Climate Model (WACCM) Model Output, Research Data Archive at the National Center for Atmospheric Research, Computational and Information System Laboratory, 2020, https://doi.org/10.5065/G643-Z138, (last access: 05 December 2022).

Beirle, S., Hörmann, C., Jöckel, P., Liu, S., Penning De Vries, M., Pozzer, A., Sihler, H., Valks, P. and Wagner, T.: The STRatospheric Estimation Algorithm from Mainz (STREAM): Estimating stratospheric NO2 from nadir-viewing satellites by weighted convolution, Atmos. Meas. Tech., 9(7), 2753–2779, doi:10.5194/amt-9-2753-2016, 2016.

Boersma, K. F., Eskes, H. J. and Brinksma, E. J.: Error analysis for tropospheric NO2 retrieval from space, J. Geophys. Res. Atmos., 109(4), doi:10.1029/2003jd003962, 2004.

https://doi.org/10.5194/amt-2024-33
Preprint. Discussion started: 12 March 2024

Bovensmann, H., Burrows, J. P., Buchwitz, M., Frerick, J., Noël, S., Rozanov, V. V., Chance, K. V., and Goded, A. P. H., SCIAMACHY: Mission Objectives and Measurement Modes, *J. Atmos. Sci.*, 56, 127-150, 1999, https://doi.org/10.1175/1520-0469(1999)056<0127:SMOAMM>2.0.CO;2.

Buchholz, R. R., Emmons, L. K., Tilmes, S., and The CESM2 Development Eam, CESM2.1/CAM-Chem Instantaneous Output for Boundary Conditions, UCAR/NCAR – Atmospheric Chemistry Observations and Modeling Laboratory, Lat: -5 to 45, Lon: 75 to 145, 28 Nov 2022, 2019, https://doi.org/10.5065/NMP7-EP60.

Burrows, J. P., Weber, M., Buchwitz, M., Rozanov, V., Ladstätter-Weißenmayer, A., Richter, A., DeBeek, R., Hoogen, R., Bramstedt, K., Eichmann, K.-U., Elsinger, M., and Perner, D., The Global Ozone Monitoring Experiment (GOME): Mission Concept and First Scientific Results, *J. Atmos. Sci.*, 56, 151-175, 1999, https://doi.org/10.1175/1520-0469(1999)056<0151:TGOMEG>2.0CO;2.

Crippa, M. Guizzardi, D., Butler, T., Keating, T., Wu, R., Kaminski, J., Kuenen, J., Kurokawa, J., Chatani, S., Morikawa, T., Pouliot, G., Racine, J., Moran, M. D., Klimont, Z., Manseau, P. M., Mashayekhi, R., Henderson, B. H., Smith, S. J., Suchyta, H., Muntean, M., Solazzo, E., Banja, M., Schaaf, E., Pagani, F., Woo, J.-H., Kim, J., Monforti-Ferrario, F., Pisonim E., Zhang, J., Niemi, D., Sassi, M., Ansari, T., and Foley, K., The HTAP_v3 emission mosaic: merging regional and global monthly emissions (2000-2018) to support air quality modeling and policies, *Earth Syst. Sci. Data*, 15, 2667-2694, 2023, https://doi.org/10.5194/essd-15-2667-2023.

Crippa Monica, HTAP_v3 emission mosaic [edgar_HTAPv3_2018_*], Zenodo, 2023, https://doi.org/10.5281/zenodo.7516361.

Emmons, L. K., Walters, S., Hess, P. G., Lamarque, J.-F., Pfister, G. G., Fillmore, D., Granier, C., Guenther, A., Kinnison, D., Laepple, T., Orlando, J., Tie, X., Tyndall, G.,

https://doi.org/10.5194/amt-2024-33
Preprint. Discussion started: 12 March 2024

Weidinmyer, C., Baughcum, S. L., and Kloster, S., Description and evaluation of the Model for Ozone and Related chemical Tracers, version 4 (MOZART-4), *Geosci. Model Dev.*, 3, 43-67, 2010, https://doi.org/10.5194/gmd-3-43-2010.

Emmons, L. K., Schwantes, R. H., Orlando, J. J., Tyndall, G., Kinnison, D., Lamarque, J.-F., Marsh, D., Mills, M. J., Tilmes, S., Bardeen, C., Buchholz, R. R., Conley, A., Gettelman, A., Garcia, R., Simpson, I., Blake, D. R., Meinardi, S., and Pétron, G., The Chemistry Mechanism in the Community Earth System Model Version 2 (CESM2), *Journal of Advances in Modeling Earth Systems*, 12, e2019MS001882, 2020, https://doi.org/10.1029/2019MS001882.

Eskes, J., van Geffen, J., Boersma, F., Eichmann, K.-U., Apituley, A., Pedergnana, M., Sneep, M., Veefkind, J. P., and Loyola, D., Sentinel-5 precursor/TROPOMI Level 2 Product User Manual Nitrogendioxide, Tech. rep., Report S5P-KNMI-L2-0021-MA, issue 4.1.0, 11 July 2022, ESA, 2022, https://sentinel.esa.int/web/sentinel/technical-guides/sentinel-5p/products-algorithms (last access: 26 February 2024).

Grell, G. A., Peckham, S. E., Schmitz, R., McKeen, S. A., Frost, G., Shamarock, W. C., and Eder B., Fully coupled "online" chemistry within the WRF model, *Atmos. Environ.*, 39, 6957-6975, 2005, https://doi.org/10.1016/j.atmosenv.2005.04.027.

Heimann, M., Monfray, P., and Polian, G., Long-range transport of 222Rn- a test for 3D tracer models, *Chem. Geol.*, 70, 98-98, 1988.

Hong, H., Lee, H., Kim, J., Jeong, U., Ryu, J., Lee, D. S., Investigation of Simultaneous Effects of Aerosol Properties and Aerosol Peak Height on the Air Mass Factors for Space-Borne NO_2 Retrievals, *remote sens.*, 9(3), 208, 2017, https://doi.org/10.3390/rs9030208.

Huijnen, V., Williams, J., van Weele, M., van Noije, T., Krol, M., Dentener, F., Segers, A., Houweling, S., Peters, W., de Laat, J., Boersma, F., Bergamaschi, P., van Velthoven, P., Le Sager, P., Eskes, H., Alkemade, F., Scheele, R., Nédélec, P., and

https://doi.org/10.5194/amt-2024-33
Preprint. Discussion started: 12 March 2024

Atmospheric Measurement Techniques Discussions

Pätz, H.-W., The global chemistry transport model TM5: description and evaluation of the tropospheric chemistry version 3.0, *Geosci. Model Dev.*, 3, 445-473, 2010, https://doi.org/10.5194/gmd-3-445-2010.

Kim, H. C., Kim, S., Lee, S.-H., Kim, B.-U., and Lee, P., Fine-Scale Columnar and Surface NO_x concentrations over South Korea: Comparison of Surface Monitors, TROPOMI, CMAQ and CAPSS Inventory, *Atmosphere*, 11, 101, 2020, https://doi.org/10.3390/atmos11010101.

Kim, J., Jeong, U., Ahn, M.-H., Kim, J. H., Park, R. J., Lee, H., Song, C. H., Choi, Y.-S., Lee, K.-J., Yoo, J.-M., Jeong, M.-J., Park, S. K., Lee, K.-M., Song, C.-K., Kim, S.-W., Kim, Y. J., Kim, S.-W., Kim, M., Go, S., Liu, X., Chance, K., Miller, C. C., Al-Saadi, J., Veihelmann, B., Bhartia, P. K., Torres, O., González Abad, G., Haffner, D. P., Ko, D. H., Lee, S. H., Woo, J.-H., Chong, H., Park, S. S., Nicks, D., Choi, W. J., Moon, K.-J., Cho, A., Yoon, J., Kim, S.-K., Hong, H., Lee, K., Lee, H., Lee, S., Choi, M., Veekfind, P., Levelt, P. F., Edwards, D. P., Kang, M., Eo, M., Bak, J., Baek, K., Kwon, H.-A., Yang, J., Park, J., Han, K. M., Kim, B.-R., Shin, H.-W., Choi, H., Lee, E., Chong, J., Cha, Y., Koo, J.-H., Irie, H., Hayashida, S., Kasai, Y., Kanaya, Y., Liu, C., Lin, J., Crawford, J. H., Carmichael, G. R., Newchurch, M. J., Lefer, B. L., Herman, J. R., Swap, R. J., Lau, A. K. H., Kurosu, T. P., Jaross, G., Ahlers, B., Dobber, M., McElroy, C. T., and Choi, Y., New Era of Air Quality Monitoring from Space: Geostationary Environment Monitoring Spectrometer (GEMS), *Bull. Amer. Meteor. Soc.*, 101, E1-E22, 2020, https://doi.org/10.1175/BAMS-D-18-0013.1.

Kim, K.-M., Kim, S.-W., Seo, S., Blake, D. R., Cho, S., Crawford, J. H., Emmons, L., Fried, A., Herman, J. R., Hong, J., Jung, J., Pfister, G., Weinheimer, A. J., Woo, J.-H., Zhang, Q., Sensitivity of the WRF-Chem v4.4 ozone, formaldehyde, and precursor simulations to multiple bottom-up emission inventories over East Asia during the KORUS-AQ field campaign, *Geosci. Model Dev. Disc.*, 2023, https://doi.org/10.5194/gmd-2023-132.

https://doi.org/10.5194/amt-2024-33
Preprint. Discussion started: 12 March 2024

Kim, S.-W., McDonald, B. C., Brown, S. S., Dube, B., Ferrare, R. A., Frost, G. J., Harley, R. A., Holloway, J. S., Lee, H.-J., McKeen, S. A., Neuman, J. A., Nowak, J. B., Oetjen, H., Ortega, I., Pollack, I. B., Roberts, J. M., Ryerson, T. B., Scarino, A. J., Senff, C. J., Thalman, R., Trainer, M., Volkamer, R., Wagner, N., Washenfelder, R. A., Waxman, E., and Young, C. J., Modeling the weekly cycle of NO_x and CO emissions and their impacts on O_3 in the Los Angeles-South Coast Air Basin during the CalNex 2010 field campaign, *J. Geophys. Res. Atmos.*, 121, 1340-1360, 2016, https://doi.org/10.1002/2015JD024292.

Kleipool, Q. L., Dobber, M. R., de Haan, J. F., and Levelt, P. F., Earth surface reflectance climatology from 3 years of OMI data, *J. Geophys. Res. Atmos.*, 113, D18308, 2008, https://doi.org/10.1029/2008JD010290.

Levelt, P. F., van den Oord, G. H. J., Dobber, M., R., Mälkki, A., Visser, H., de Vries, J., Stammes, P., Lundell, J. O. V., Saari, H., The Ozone Monitoring Instrument, *IEEE Trans. Geosci. Remote Sens.*, 44(5), 1093-1101, 2006, https://doi.org/10.1109/TGRS.2006.872333.

Lorente, A., Boersma, K. F., Yu, H., Dörner, S., Hilboll, A., Richter, A., Liu, M., Lamsal, L. N., Barkley, M., De Smedt, I., Van Roozendael, M., Wang, Y., Wagner, T., Beirle, S., Lin, J.-T., Krotkov, N., Stammes, P., Wang, P., Eskes, H. J., and Krol, M., Structural uncertainty in air mass factor calculation for NO_2 and HCHO satellite retrievals, *Atmos. Mech. Tech.*, 10, 759-782, 2017, https://doi.org/10.5194/amt-10-759-2017.

Oak, Y. J., Jacob, D. J., Balasus, N., Yang, L. H., Chong, H., Park, J., Lee, H., Lee, G. T., Ha, E. S., Park, R. J., Kwon, H.-A., and Kim, J., A bias-corrected GEMS geostationary satellite product for nitrogen dioxide using machine learning to enforce consistency with the TROPOMI satellite instrument, *in preparation*, https://acmg.seas.harvard.edu/sites/projects.iq.harvard.edu/files/acmg/files/manuscript.pdf.

https://doi.org/10.5194/amt-2024-33
Preprint. Discussion started: 12 March 2024

Palmer, P. I., Jacob, D. J., Chance, K., Martin, R. V., Spurr, R. J. D., Kurosu, T. P., Bey, I., Yantosca, R., Fiore, A., and Li, Q., Air mass factor formulation for spectroscopic measurements from satellites: Application to formaldehyde retrievals from the Global Ozone Monitoring Experiment, *J. Geophys. Res.*, 106, 14539-14550, 2001, https://doi.org/10.1029/2000JD900772.

Richter et al., An improved tropospheric NO_2 retrieval for GEMS, manuscript in preparation, 2024.

Rozanov, V. V., Rozanov, A. V., Kokhanovsky, A. A. and Burrows, J. P.: Radiative transfer through terrestrial atmosphere and ocean: Software package SCIATRAN, J. Quant. Spectrosc. Radiat. Transf., 133, 13–71, doi:10.1016/j.jqsrt.2013.07.004, 2014.

Shah, V., Jacob, D. J., Li, K., Silvern, R. F., Zhai, S., Liu, M., Lin, J., and Zhang, Q., Effect of changing NOx lifetime on the seasonality and long-term trends of satellite-observed tropospheric NO2 columns over China, *Atmos. Chem. Phys.*, 20, 1483-1495, 2020, https://doi.org/10.5194/acp-20-1483-2020.

Skamarock, W. C., Klemp, J. B., Dudhia, J., Gill, D. O., Liu, Z., Berner, J., Wang, W., Powers, J. G., Duda, M. G., Barker, D. M., Huang, X.-Y., A Description of the Advanced Research WRF Model Version 4 (No. NCAR/TN-556+STR), 2021, https://doi.org/10.5065/1dfh-6p97.

van Geffen, J., Eskes, H., Compernolle, S., Pinardi, G., Verhoelst, T., Lambert, J.-C., Sneep, M., ter Linden, M., Ludewig, A., Boersma, K. F., and Veefkind, J. P., Sentinel-5P TROPOMI NO2 retrieval: impact of version v2.2 improvements and comparisons with OMI and ground-based data, *Atmos. Meas. Tech.*, 15, 2037-2060, 2022, https://doi.org/10.5194/amt-15-2037-2022.

Veefkind, J. P., Aben, I., McMullan, K. Förster, H., de Vries, J., Otter, G., Claas, J., Eskes, H. J., de Haan, J. F., Kleipool, Q., van Weele, M., Hasekamp, O., Hoogeveen, R., Landgraf, J., Snel, R., Tol, P., Ingmann, P., Voors, R., Kruizinga, B., Vink, R.,

https://doi.org/10.5194/amt-2024-33
Preprint. Discussion started: 12 March 2024

Atmospheric Measurement Techniques Discussions

Visser, H., and Levelt, P. F., TROPOMI on the ESA Sentinel-5 Precursor: A GMES mission for global observations of the atmospheric composition for climate, air quality and ozone layer applications, *Remote Sens. Environ.*, 120, 70-83, 2012, https://doi.org/10.1016/j.rse.2011.09.027.

Williams, J. E., Boersma, K. F., Le Sager, P., and Verstraeten, W. W.: The high-resolution version of TM5-MP for optimized satellite retrievals: description and validation, Geosci. Model Dev., 10, 721–750, https://doi.org/10.5194/gmd-10-721-2017, 2017.

Yang, L. H., Jacob, D. J., Dang, R., Oak, Y. J., Lin, H., Kim, J., Zhai, S., Colombi, N. K., Pendergrass, D. C., Beaudry, E., Shah, V., Feng, X., Yantosca, R. M., Chong, H., Park, J., Lee, H., Lee, W.-J., Kim, S., Kim, E., Travis, K. R., Crawford, J. H., Liao, H., Interpreting GEMS geostationary satellite observations of the diurnal variation of nitrogen dioxide (NO_2) over East Asia, *EGUsphere [preprint]*, 2023, https://doi.org/10.5194/egusphere-2023-2979.

https://doi.org/10.5194/amt-2024-33
Preprint. Discussion started: 12 March 2024

Atmospheric Measurement Techniques Discussions

List of Tables

Table 1. Experimental settings of WRF-Chem model simulations.

https://doi.org/10.5194/amt-2024-33
Preprint. Discussion started: 12 March 2024

Atmospheric Measurement Techniques Discussions

List of Figures

Figure 1. Diurnal variations of GEMS NO_2 TropVCD in January, April, July, and October 2021 with *a priori* data of WRF-Chem v3 (red solid) and TM5 (blue solid) over SMA. Shades indicate 1-sigma (σ) bound from each of the mean values.

Figure 2. Spatial maps for differences of GEMS NO_2 TropVCD between using *a priori* data of WRF-Chem v3 and TM5 in January, April, July, and October. The pink box shown in the upper-left figure indicates the SMA domain.

Figure 3. Diurnal variations of model-simulated NO_2 TropVCD in January, April, July, and October 2021 from WRF-Chem v3 (red solid) and TM5 (blue solid) over SMA. Shades indicate 1-sigma (σ) bound from each of the mean values.

Figure 4. Curtain plots of model vertical NO_2 profiles from WRF-Chem v3 (upper row) and TM5 (lower row) in January, April, July, and October 2021 over SMA.

Figure 5. Diurnal variations of GEMS NO_2 TropVCD with *a priori* data of WRF-Chem v2 (red solid), WRF-Chem f2 (yellow solid), and WRF-Chem v3 (blue solid) during October 25 – 28, 2021 over SMA. Shades indicate 1-sigma (σ) bound from each of the mean values.

Figure 6. Diurnal variations of model-simulated NO_2 TropVCD from WRF-Chem v2 (red solid), WRF-Chem f2 (yellow solid), and WRF-Chem v3 (blue solid) during October 25 – 28, 2021 over SMA. Shades indicate 1-sigma (σ) bound from each of the mean values.

Figure 7. Diurnal variations of air mass factors from WRF-Chem v2 (red solid), WRF-Chem f2 (yellow solid), and WRF-Chem v3 (blue solid) during October 25 – 28, 2021 over SMA.

Figure 8. Diurnal variations of air mass factors in January, April, July, and October 2021 from WRF-Chem v3 (red solid) and TM5 (blue solid) over SMA.

https://doi.org/10.5194/amt-2024-33
Preprint. Discussion started: 12 March 2024

Atmospheric Measurement Techniques Discussions

Table 1. Experimental settings of WRF-Chem model simulations.

Case name	Description
WRF-Chem v2	EDGAR-HTAP v3
WRF-Chem f2	EDGAR-HTAP v3, using profiles of 04:45 UTC (13:45 KST) only
WRF-Chem v3	EDGAR-HTAP v3 with 20% reduced NO_x emissions for whole domain

https://doi.org/10.5194/amt-2024-33
Preprint. Discussion started: 12 March 2024

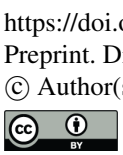

Atmospheric Measurement Techniques Discussions

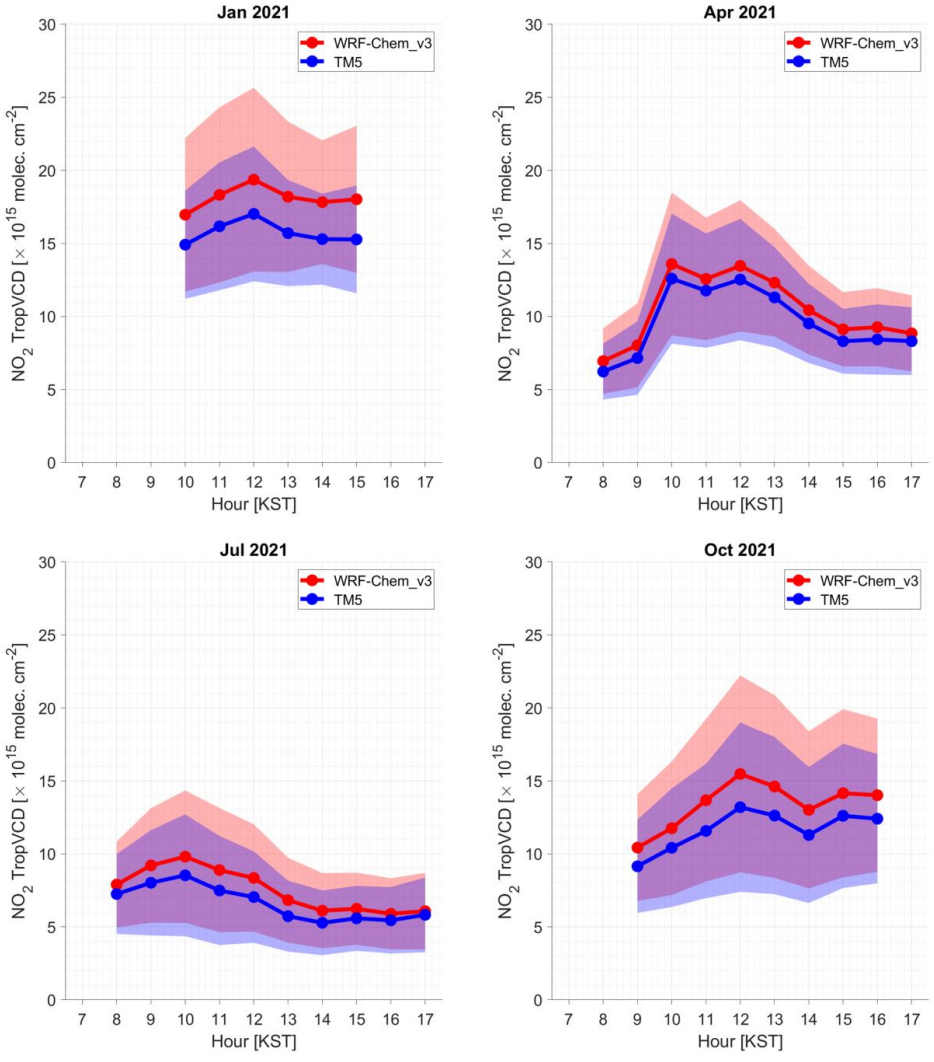

Figure 1. Diurnal variations of GEMS NO_2 TropVCD in January, April, July, and October 2021 with *a priori* data of WRF-Chem v3 (red solid) and TM5 (blue solid) over SMA. Shades indicate 1-sigma (σ) bound from each of the mean values.

https://doi.org/10.5194/amt-2024-33
Preprint. Discussion started: 12 March 2024

Atmospheric Measurement Techniques Discussions

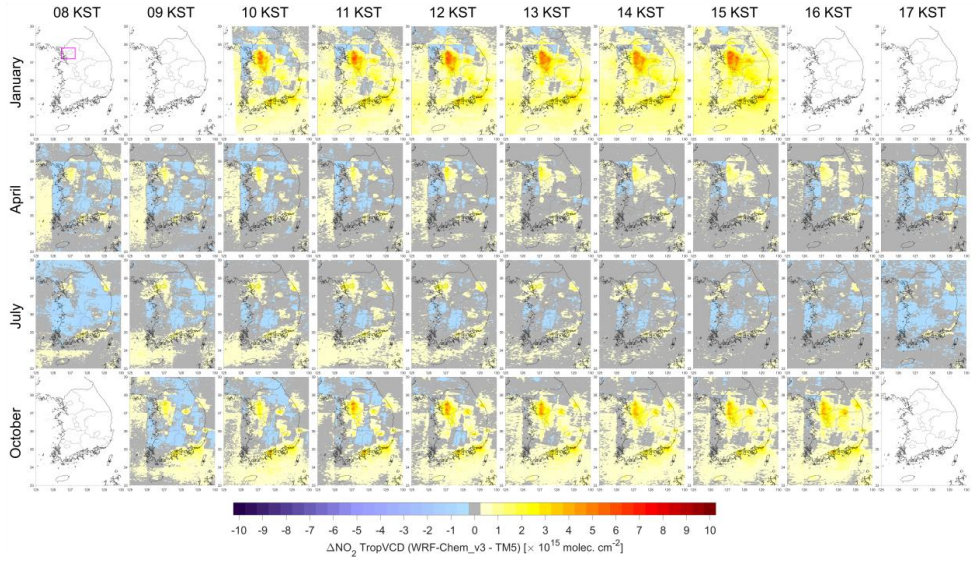

Figure 2. Spatial maps for differences of GEMS NO_2 TropVCD between using *a priori* data of WRF-Chem v3 and TM5 on January, April, July, and October. The pink box shown in the upper-left figure indicates the SMA domain.

https://doi.org/10.5194/amt-2024-33
Preprint. Discussion started: 12 March 2024

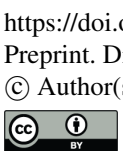

Atmospheric Measurement Techniques Discussions

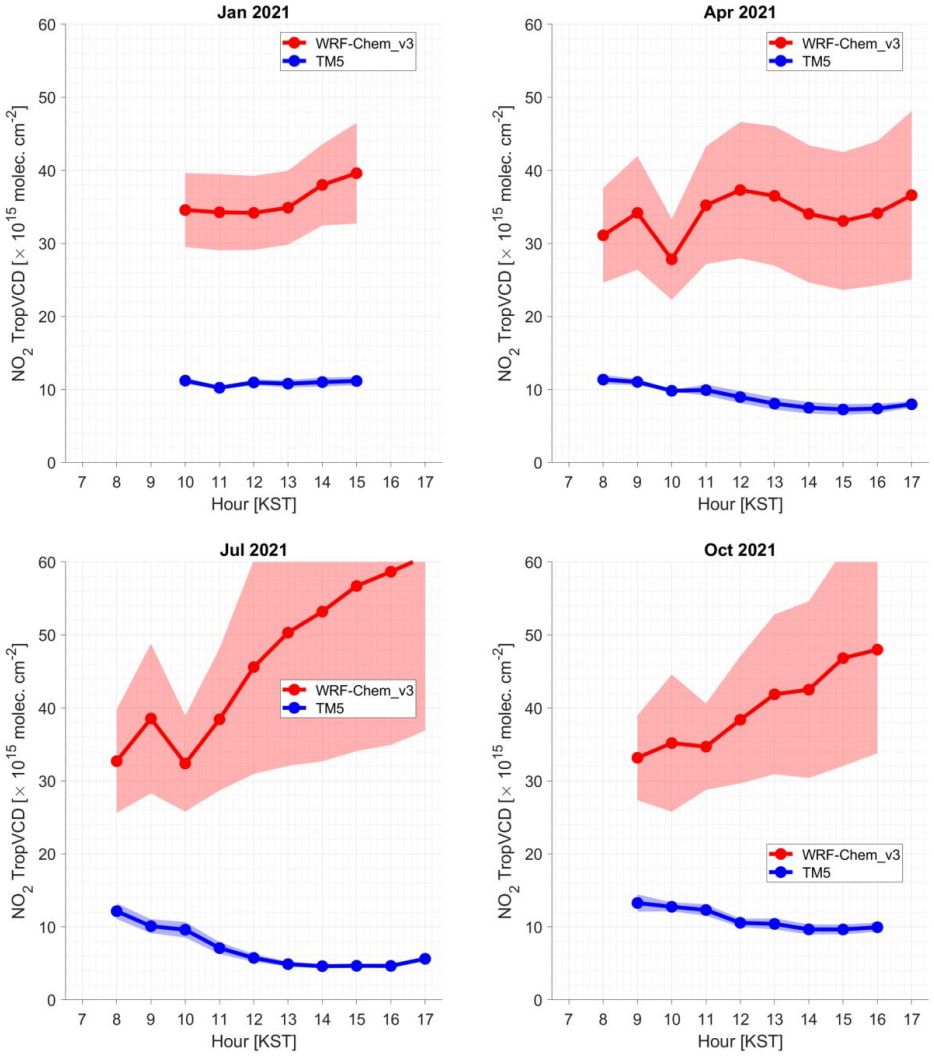

Figure 3. Diurnal variations of model-simulated NO_2 TropVCD in January, April, July, and October 2021 from WRF-Chem v3 (red solid) and TM5 (blue solid) over SMA. Shades indicate 1-sigma (σ) bound from each of the mean values.

https://doi.org/10.5194/amt-2024-33
Preprint. Discussion started: 12 March 2024

Atmospheric Measurement Techniques Discussions

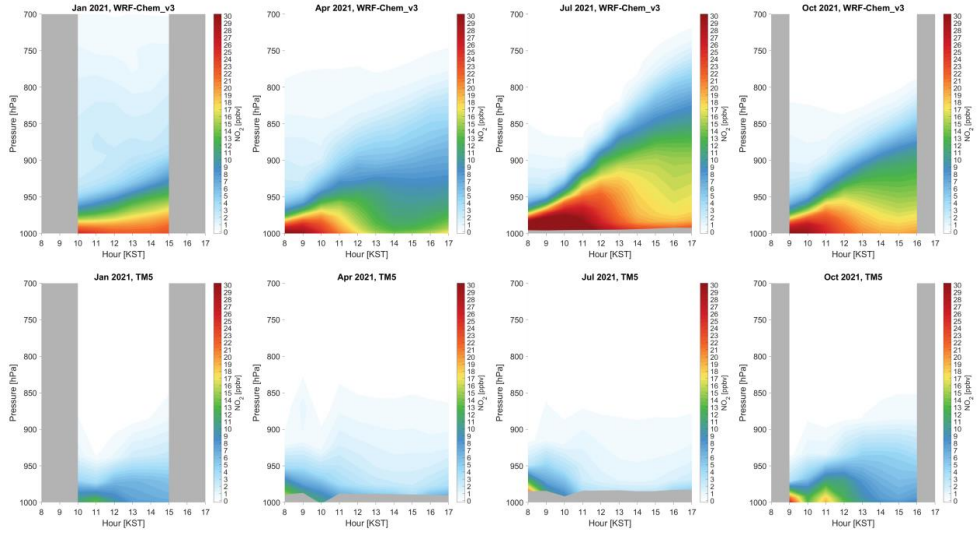

Figure 4. Curtain plots of model vertical NO_2 profiles from WRF-Chem v3 (upper row) and TM5 (lower row) in January, April, July, and October 2021 over SMA.

https://doi.org/10.5194/amt-2024-33
Preprint. Discussion started: 12 March 2024

Atmospheric Measurement Techniques Discussions

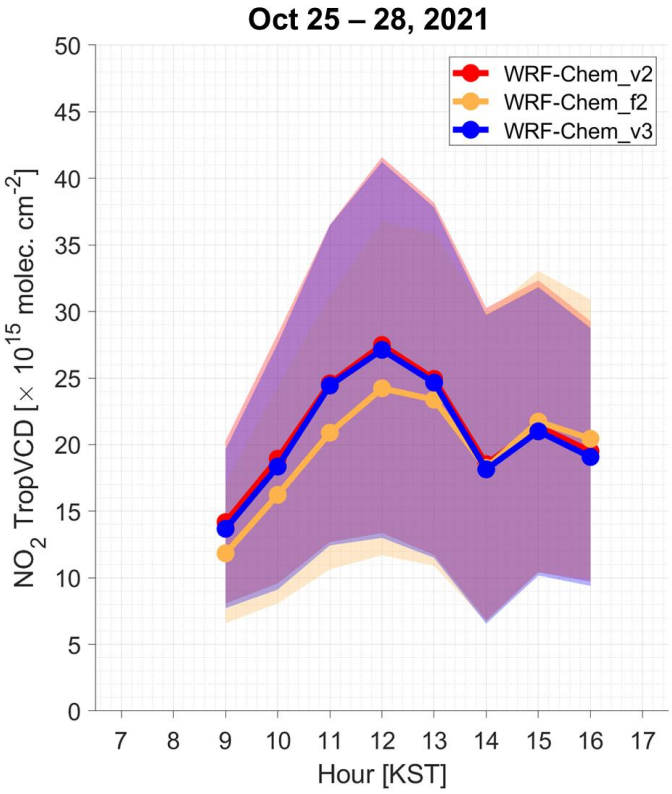

Figure 5. Diurnal variations of GEMS NO_2 TropVCD with *a priori* data of WRF-Chem v2 (red solid), WRF-Chem f2 (yellow solid), and WRF-Chem v3 (blue solid) during October 25 – 28, 2021 over SMA. Shades indicate 1-sigma (σ) bound from each of the mean values.

https://doi.org/10.5194/amt-2024-33
Preprint. Discussion started: 12 March 2024

Atmospheric Measurement Techniques Discussions

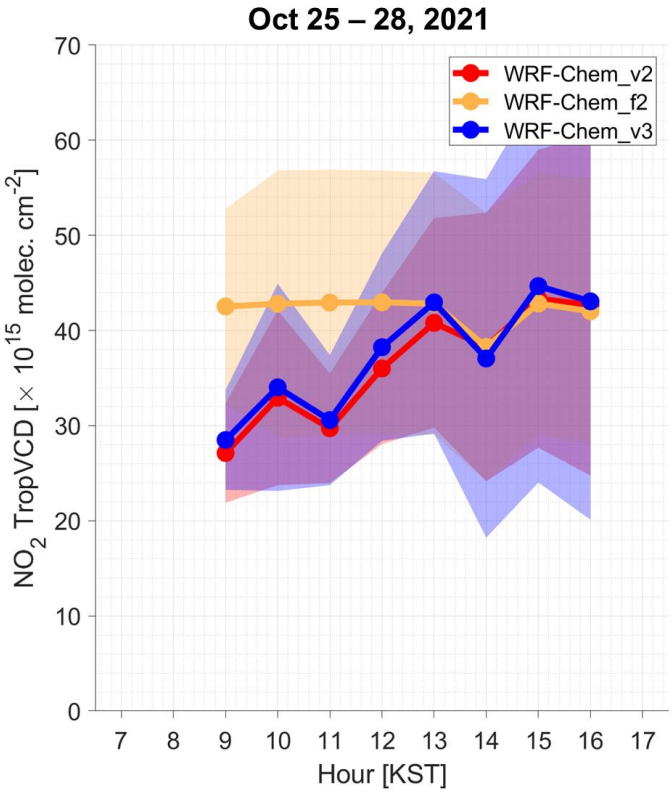

Figure 6. Diurnal variations of model-simulated NO_2 TropVCD from WRF-Chem v2 (red solid), WRF-Chem f2 (yellow solid), and WRF-Chem v3 (blue solid) during October 25 – 28, 2021 over SMA. Shades indicate 1-sigma (σ) bound from each mean values.

https://doi.org/10.5194/amt-2024-33
Preprint. Discussion started: 12 March 2024

Atmospheric Measurement Techniques Discussions

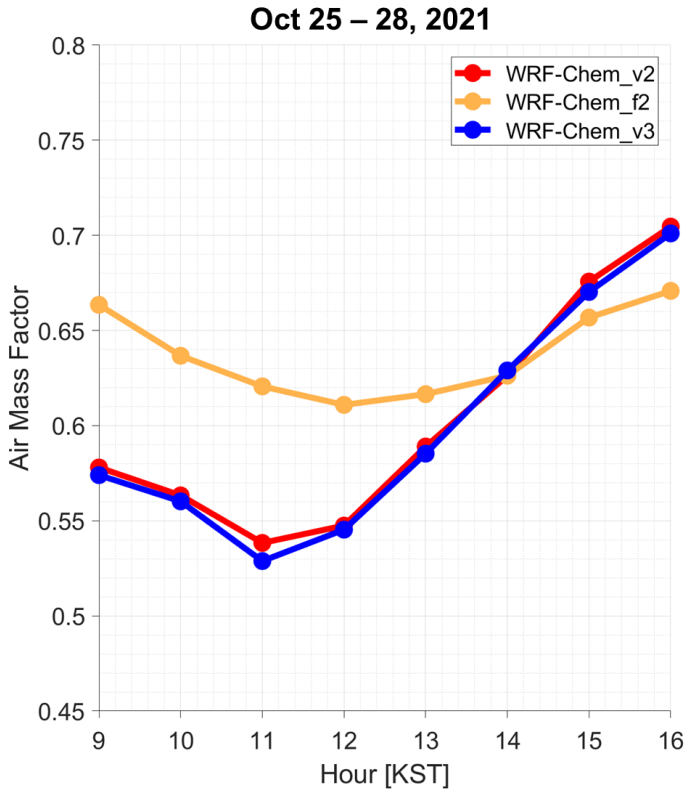

Figure 7. Diurnal variations of air mass factors from WRF-Chem v2 (red solid), WRF-Chem f2 (yellow solid), and WRF-Chem v3 (blue solid) during October 25 – 28, 2021 over SMA.

https://doi.org/10.5194/amt-2024-33
Preprint. Discussion started: 12 March 2024

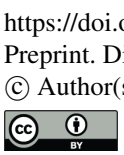

Atmospheric Measurement Techniques Discussions

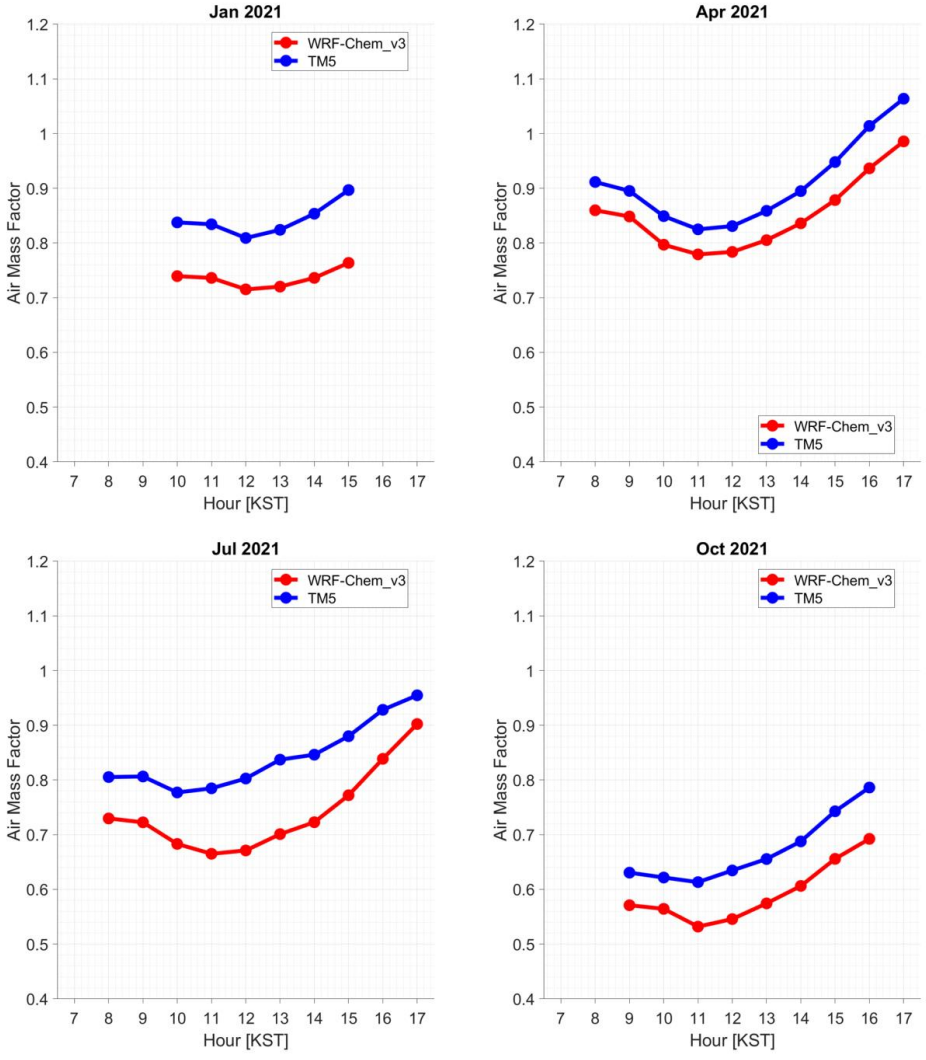

Figure 8. Diurnal variations of air mass factors on January, April, July, and October 2021 from WRF-Chem v3 (red solid) and TM5 (blue solid) over SMA.